Optics Letters

Extreme amplitude spikes in a laser model described by the complex Ginzburg–Landau equation

Wonkeun Chang,[1,*] Jose M. Soto-Crespo,[2] Peter Vouzas,[1] and Nail Akhmediev[1]

[1]Optical Sciences Group, Research School of Physics and Engineering, The Australian National University, Acton ACT 2601, Australia
[2]Instituto de Óptica, C.S.I.C., Serrano 121, 28006 Madrid, Spain
*Corresponding author: wonkeun.chang@anu.edu.au

Received 14 April 2015; revised 28 May 2015; accepted 29 May 2015; posted 1 June 2015 (Doc. ID 237904); published 16 June 2015

We have found new dissipative soliton in the laser model described by the complex cubic-quintic Ginzburg–Landau equation. The soliton periodically generates spikes with extreme amplitude and short duration. At certain range of the equation parameters, these extreme spikes appear in pairs of slightly unequal amplitude. The bifurcation diagram of spike amplitude versus dispersion parameter reveals the regions of both regular and chaotic evolution of the maximal amplitudes.

OCIS codes: (060.5530) Pulse propagation and temporal solitons; (140.7090) Ultrafast lasers; (320.7110) Ultrafast nonlinear optics.

http://dx.doi.org/10.1364/OL.40.002949

The concept of dissipative soliton [1] helps to understand and to model passively mode-locked lasers [2]. It serves as a useful tool for the description of various modes of laser operation [2] and even for prediction of new effects [3]. The most common mathematical implementation of a dissipative system is the complex cubic-quintic Ginzburg–Landau equation [2]. Despite its deceptive simplicity, this equation admits highly complicated solutions. The complexity of its solutions literally created the world of the Ginzburg–Landau equation [4]. One of the reasons for such complexity is that this equation has several free parameters. Changing just one of them by a small amount may dramatically change the nature of the solution. Here, we are interested only in localized solutions, i.e., dissipative solitons [1]. A plethora of different types of dissipative solitons have been studied so far: stationary solitons [5,6], pulsating solitons [7,8], exploding solitons [9], creeping solitons [3,10], composite solitons [11,12], and multisolitons [13,14]. Our present work shows that the list is still far from being complete.

The analysis of the whole set of parameters where soliton solutions can be found is a tedious task. Sophisticated searching numerical schemes such as the one described in the recent work [15] may help to some extent, but still there is always the possibility of missing interesting regimes. Here we have found numerically a regime of pulse generation that is characterized by an extreme growth of the pulse amplitude. The most impressive feature of this regime is that the process happens in a self-organized manner, and hence any localized initial profile reasonably close to the solution converges to it.

So far, there have been two models predicting the existence of waves with extreme amplitudes in dissipative systems [16,17]. They are both lumped models. The one developed in [16] relates the generation of very-high-amplitude pulses to the multiple collision of several dissipative solitons coexisting in the cavity. This model has been verified experimentally in mode-locked fiber lasers [18,19]. The model developed in [17] operates with pulses that evolve chaotically in the cavity and, occasionally, may reach much higher amplitudes than the average amplitude of the evolving pulses. This last model corresponds approximately to the experimental observations made in Ti:sapphire lasers [20,21]. There are currently no studies of distributed models predicting the existence of a single pulse that can reach extremely high amplitudes. The present work fills this gap.

For the passively mode-locked laser model, we apply the master-equation approach that was first introduced in the pioneering work by Hermann Haus [22]. Namely, we use the cubic-quintic complex Ginzburg–Landau equation, which in its standard form reads [2]

$$i\psi_z + \frac{D}{2}\psi_{tt} + |\psi|^2\psi + \nu|\psi|^4\psi = i\delta\psi + i\epsilon|\psi|^2\psi + i\beta\psi_{tt} + i\mu|\psi|^4\psi, \tag{1}$$

where t is the normalized time in a frame of reference moving with the group velocity, ψ is the complex envelope of the optical field, and z is the propagation distance along the unfolded cavity. On the left-hand side, D denotes the cavity dispersion, being anomalous when $D > 0$ and normal if $D < 0$, and ν is the quintic refractive index coefficient. Dissipative terms are written on the right-hand side of (1) where δ denotes linear gain/loss, β is the gain bandwidth coefficient, and ϵ and μ are the cubic and quintic gain/loss coefficients, respectively. Although Eq. (1) is an approximate general model, most of its known stable solutions so far have been reported experimentally in various mode-locked laser configurations.

For the numerical simulations, we used two different programs in three different computing platforms to verify that the results presented here are correct. We implemented a split-step technique with a fourth-order Runge–Kutta algorithm for solving the nonlinear part of the equation, while the linear part was solved in Fourier space. Modifications of this technique [23] were also used. The step sizes were made small enough in both z and t directions to correctly represent the parts of the solution with sharply growing amplitudes. Namely, we used up to 524,288 mesh points in transverse direction to sample the t-interval of up to $[-200, 200]$ which is sufficiently large to have practically zero values of the envelope function at its edges. The spectrum of the localized solutions are also well sampled in Fourier domain with this choice. In the longitudinal direction, we used typically a step length of 10^{-6}, although the use of an adaptive step-size method allowed to consider bigger step sizes too. All solutions presented below have fairly large basin of attraction, i.e., a wide range of initial conditions converges to these solutions. Initial condition that is not the solution evolves first with strong modulations before it reached the solution.

By solving Eq. (1) numerically for the set of parameters given in the caption of Fig. 1, we have found quite unusual pulsations of a single pulse. Namely, they lead to a sharp growth of the amplitude of the pulse followed by an even sharper drop. The lifetime of the extra-high-amplitude part of the pulse is significantly shorter than the period of pulsations. The amplitude of the pulse in this part is also much higher than the amplitude of the pedestal, which is around 15. A second extreme growth, slightly different, immediately follows the first one, while

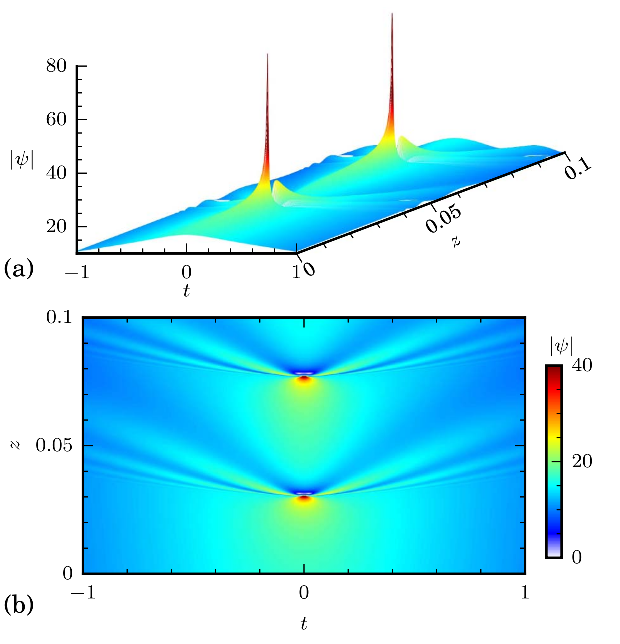

Fig. 1. Extreme pulses found for the following set of Eq. (1) parameters: $D = -2.5$, $\nu = -0.002$, $\delta = -0.08$, $\beta = 0.18$, $\epsilon = 0.04$, and $\mu = -0.000025$. Extreme pulses are located on top of a wider pulse, which acts as its pedestal. Only the central part of the pulse is shown here. Panel (a) shows the 3-dimensional evolution. Note that the vertical scale starts from 10. Panel (b) gives the same data in false color. The color scale is saturated at 40 to show the spike which otherwise would not be visible.

the situation remains basically stationary in the rest of the period. For the above equation parameters the spikes appear as asymmetric pairs as shown in Fig. 1.

This figure allows us to appreciate the dramatic increase of the pulse amplitude at two points of evolution. The sharp growth can be considered as unexpected, as during most of the period, the pulse amplitude varies slightly, remaining near 15. We can refer to this part of the pulse as *pedestal*. The width of the extreme pulse is much narrower than the width of the pedestal. The two red spots in Fig. 1(b) represent the two extreme pulses forming the pair. After the sharp growth up to the maximal value, the central amplitude sharply drops to a value ≈ 2 which is much lower than the average amplitude of the pedestal. It is even more surprising that the extreme pulse generation is repeated after a short interval following the first peak.

The whole evolution is periodic with two extreme maxima in each period. Figure 2 shows the evolution of the soliton amplitude at its center (red solid-line), i.e., at the point $t = 0$, and the total pulse energy $Q(z)$ which is $\int_{-\infty}^{\infty} |\psi(z, t)|^2 dt$ (black dashed-line). The amplitudes of the two extreme peaks are comparable but not exactly the same. The first peak is slightly higher than that of the second one. Accordingly, the total energy when the second peak appears is lower than that of the first one. The major fraction of the energy is contained within the pedestal. The increase of energy when the first extreme pulse appears is around 30% of the average energy of the pulse. The pulse energy increases gradually well before the appearance of the first spike as shown in Fig. 2. The period of pulsations is much longer than the lifetime of each peak. It is also longer than the delay between the two peaks. The pair generation is repeated indefinitely.

Another observation from Fig. 2 is that the amplitude of the extreme peaks in the solution are approximately 5 times higher than the amplitude of the pedestal. This means that the intensity amplification of the peak is around 25. This creates interesting possibilities for practical applications of this effect. A single laser oscillator can be used for generating high-amplitude ultra-short pulses without additional compressors provided that the correct parameters of the system are found and carefully tuned to match the period of its evolution with the cavity length. According to our simulations, this can be done in lasers with normal average cavity dispersion.

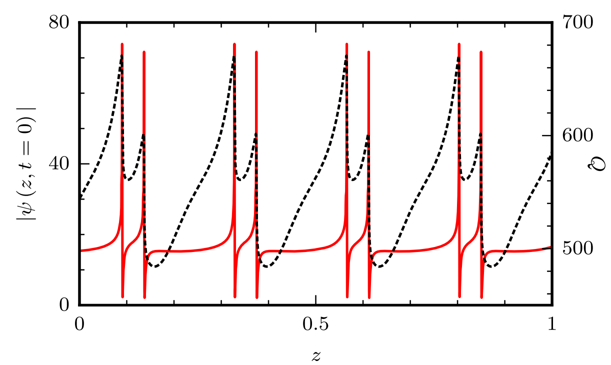

Fig. 2. Evolution of the pulse amplitude at its center $|\psi(z, t = 0)|$ (red solid-line) and the pulse energy $Q(z)$ (black dashed-line) for the same parameters as in Fig. 1.

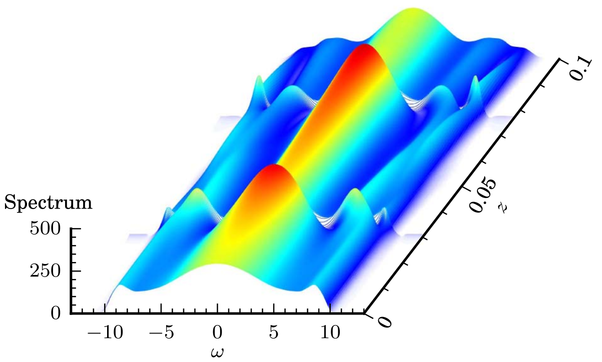

Fig. 3. Evolution of the spectrum of the pulse shown in Fig. 1.

The evolution of the pulse spectrum is shown in Fig. 3. The z-interval of this plot is the same as in Fig. 1. It includes the two extreme peaks of the pair. The extreme peaks cause the widening of the spectrum. Two sidebands are clearly seen on each side of the main spectral peak. They vary in size from the first peak to the second one. These sidebands are not related to the periodicity of the overall evolution. They quickly vanish when the high peaks disappear.

The presented regime of pulse generation is periodic with high accuracy. The existence of a pair of bound pulses within each period is an unusual feature of this periodic solution. As in other dissipative systems, periodic motion here should be considered as relaxation oscillations. These are usually sensitive to the parameters of the system. Changing any of them leads to drastic changes of the oscillation dynamics. Figure 4 shows the bifurcation diagram of the spike amplitude of the pulses when the dispersion parameter D is changed from −2.49 to −2.67. Let us recall that the previous figures correspond to the value $D = -2.5$. At this point we have two maximal amplitudes that are shown by two dots one above the other on this diagram. Reducing the parameter D, we observe a smooth increase of the two amplitudes.

The two spikes can be observed up to the point $D \approx -2.64$. At this point, a bifurcation causes the merging of the two spikes into one. In the interval $-2.662 < D < -2.64$, the soliton has only one spike in each period. Thus, we have a single curve on the bifurcation diagram. An example of the pulse-amplitude evolution at one point of this interval is shown in Fig. 5.

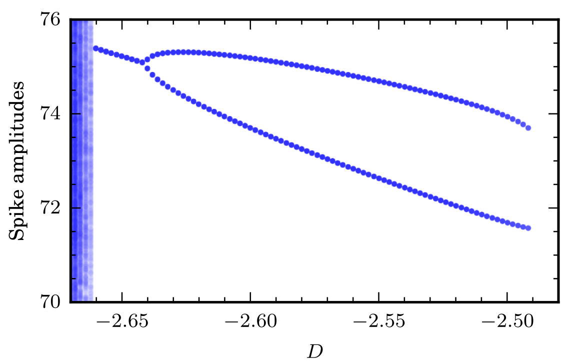

Fig. 4. Bifurcation diagram: spike amplitudes versus dispersion parameter D. Pairs merge into a single high peak at $D \approx -2.64$. The soliton becomes unstable and disappears at $D > -2.49$. The soliton enters a chaotic regime of evolution at $D < -2.662$.

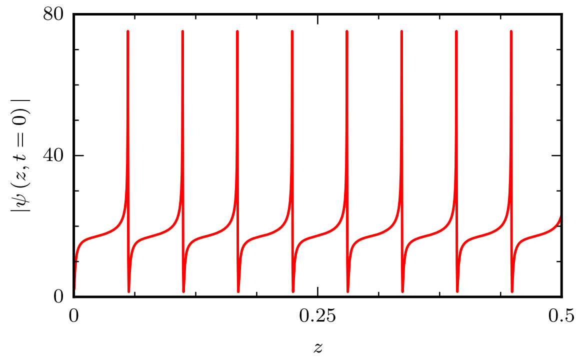

Fig. 5. Soliton central (at $t = 0$) amplitude evolution for $D = -2.65$. There is only one high peak in each period.

The point $D \approx -2.664$ represents the transition to a chaotic state where the spikes appear randomly. Every point on the vertical lines in this region represents a given realization of the peak amplitude. As the plot shows, the amplitudes here can take even higher values than in the region of regularly pulsating evolution. Thus, the region of the dispersion parameter lower than $D = -2.662$ would be the one where we can look for optical rogue waves [17,20,24,25].

We have chosen D to be variable for the bifurcation diagram, as the dispersion is the parameter of a laser system that can be changed with a relative ease. Similar bifurcation diagrams can be obtained when changing other parameters of the system. An important point is that the amplitudes of the spikes remain extremely high relative to the amplitude of the pedestal in the whole interval of D presented in Fig. 4. It also remains high when we change other parameters. For example, increasing the parameter ϵ from 0.04 to 0.042 while leaving other parameters fixed also results in the merging of the pair of peaks within a period into a single one. Still, the motion remains periodic in z, although the period changes approximately from 0.27 to 0.045, i.e., it is reduced approximately 6 times. Further increase of ϵ up to $\epsilon = 0.0423$ leads to a chaotic pulse evolution, while a small decrease of ϵ from 0.04 to $\epsilon = 0.039$ results in pulse decay and its subsequent disappearance.

In conclusion, we have found a region of parameters of the complex cubic-quintic Ginzburg–Landau equation that produces extremely high and short pulses. Although we considered a continuous model of a passively mode-locked laser, it may have an analog in the corresponding lumped model. For example, a set of design parameters can be estimated for the laser model considered in [26]. Suppose the cavity has a length of 0.6 m with an average dispersion of 0.02 $ps^2\, m^{-1}$ and nonlinear coefficient of 0.01 $W^{-1}\, m^{-1}$. Let us take the cavity gain coefficient to be 3 $dB \cdot m^{-1}$ with the 3-dB gain-bandwidth of 3.5 THz. For these given parameters, the units of the dimensionless variables t, ω, and z in our simulations correspond to 1.4 ps, 1.4π THz, and 100 m, respectively. In this regard, we should mention the laser models with injected signal [27,28]. Spiking was found to be one of the specific regimes of operation of such lasers [29,30,31]. Although the lasers with injected signal belong to a specific class of optical oscillators [32], we cannot exclude the presence of common features between their dynamics and the one based on Eq. (1). Further theoretical and experimental studies of such effects would be highly desirable, as they may provide a source of extremely high amplitude and short duration pulses from a single laser oscillator.

Australian Research Council (ARC) (DE130101432, DP140100265, DP150102057); C.A.M. (S2013/MIT-2790); Ministry of Economy and Competitiveness (MINECO) (TEC2012-37958-C02-02); Volkswagen Foundation.

J. M. S.-C. and N. A. acknowledge the support of the Volkswagen Foundation.

REFERENCES

1. N. Akhmediev and A. Ankiewicz, *Dissipative Solitons* (Springer, 2005).
2. P. Grelu and N. Akhmediev, Nat. Photonics **6**, 84 (2012).
3. N. Akhmediev, J. M. Soto-Crespo, and G. Town, Phys. Rev. E **63**, 056602 (2001).
4. I. S. Aranson and L. Kramer, Rev. Mod. Phys. **74**, 99 (2002).
5. J. M. Soto-Crespo, N. Akhmediev, and V. V. Afanasjev, J. Opt. Soc. Am. B **13**, 1439 (1996).
6. V. L. Kalashnikov and E. Sorokin, Opt. Express **22**, 30118 (2014).
7. S. C. V. Latas and M. F. S. Ferreira, Eur. Phys. J.-Spec. Top. **223**, 79 (2014).
8. D. Gomila, M. A. Matías, and P. Colet, Phys. Rev. Lett. **94**, 063905 (2005).
9. C. Cartes, O. Descalzi, and H. R. Brand, Eur. Phys. J.-Spec. Top. **223**, 2145 (2014).
10. S. C. V. Latas, M. F. S. Ferreira, and M. V. Facão, Appl. Phys. B **116**, 279 (2014).
11. V. V. Afanasjev, N. Akhmediev, and J. M. Soto-Crespo, Phys. Rev. E **53**, 1931 (1996).
12. D. S. Kharenko, O. V. Shtyrina, I. A. Yarutkina, E. V. Podivilov, M. P. Fedoruk, and S. A. Babin, J. Opt. Soc. Am. B **28**, 2314 (2011).
13. N. Akhmediev, A. Ankiewicz, and J. M. Soto-Crespo, Phys. Rev. Lett. **79**, 4047 (1997).
14. F. Sanchez, P. Grelu, H. Leblond, A. Komarov, K. Komarov, M. Salhi, A. Niang, F. Amrani, C. Lecaplain, and S. Chouli, Opt. Fiber Technol. **20**, 562 (2014).
15. S. Wang, A. Docherty, B. S. Marks, and C. R. Menyuk, J. Opt. Soc. Am. B **31**, 2914 (2014).
16. J. M. Soto-Crespo, P. Grelu, and N. Akhmediev, Phys. Rev. E **84**, 016604 (2011).
17. A. Zaviyalov, O. Egorov, R. Iliew, and F. Lederer, Phys. Rev. A **85**, 013828 (2012).
18. C. Lecaplain, P. Grelu, J. M. Soto-Crespo, and N. Akhmediev, Phys. Rev. Lett. **108**, 233901 (2012).
19. C. Lecaplain, P. Grelu, J. M. Soto-Crespo, and N. Akhmediev, J. Opt. **15**, 064005 (2013).
20. M. G. Kovalsky, A. A. Hnilo, and J. R. Tredicce, Opt. Lett. **36**, 4449 (2011).
21. A. A. Hnilo, M. G. Kovalsky, M. B. Agüero, and J. R. Tredicce, Phys. Rev. A **91**, 013836 (2015).
22. H. A. Haus, J. Appl. Phys. **46**, 3049 (1975).
23. J. Hult, J. Lightwave Technol. **25**, 3770 (2007).
24. A. F. J. Runge, C. Aguergaray, N. G. R. Broderick, and M. Erkintalo, Opt. Lett. **39**, 319 (2014).
25. J. M. Dudley, F. Dias, M. Erkintalo, and G. Genty, Nat. Photonics **8**, 755 (2014).
26. A. Zaviyalov, R. Iliew, O. Egorov, and F. Lederer, J. Opt. Soc. Am. B **27**, 2313 (2010).
27. S. Wieczorek, W. W. Chow, L. Chrostowski, and C. J. Chang-Hasnain, IEEE J. Quantum Electron. **42**, 552 (2006).
28. M. G. Zimmerman, M. A. Natiello, and H. G. Solari, Phys. D **109**, 293 (1997).
29. L. A. Lugiato, L. M. Narducci, and D. K. Bandy, Opt. Commun. **46**, 64 (1983).
30. J. R. Tredicce, F. T. Arecchi, G. L. Lippi, and G. P. Puccioni, J. Opt. Soc. Am. B **2**, 173 (1985).
31. H. G. Solari and G. L. Oppo, Opt. Commun. **111**, 173 (1994).
32. H. Li, T. L. Lucas, J. G. McInerney, M. W. Wright, and R. A. Morgan, IEEE J. Quantum Electron. **32**, 227 (2006).